Formation of Atomically Flat Silver Films on GaAs with a "Silver Mean" Quasi Periodicity

Arthur R. Smith, Kuo-Jen Chao, Qian Niu, Chih-Kang Shih*

A flat epitaxial silver film on a gallium arsenide [GaAs(110)] surface was synthesized in a two-step process. Deposition of a critical thickness of silver at low temperature led to the formation of a dense nanocluster film. Upon annealing, all atoms rearranged themselves into an atomically flat film. This silver film has a close-packed (111) structure modulated by a "silver mean" quasi-periodic sequence. The ability to grow such epitaxial overlayers of metals on semiconductors enables the testing of theoretical models and provides a connection between metal and semiconductor technologies.

An understanding of the kinetic processes that lead to flat layer-by-layer growth of epitaxial thin films (*1*) is important in fields such as quantum device engineering, where precise control of each atomic layer is desired. Much progress has been made in semiconductor-on-semiconductor and metal-on-metal epitaxy (*2*), but growing an ideal epitaxial overlayer of metal on a semiconductor has proved much more difficult to achieve. As a result of the difference in atomic bonding (metallic versus covalent or ionic) and the large disparities in surface diffusivity, metals on semiconductors tend to follow a three-dimensional (3D) growth mode (*3–5*), even for a lattice-matched system such as Fe on GaAs (*5*). Nevertheless, efforts to find such a system have continued because an ideal metal-semiconductor interface would provide a testing ground for many theoretical models (*6*).

Here, we describe a metal-on-semiconductor epitaxial system, Ag on GaAs(110), that normally follows a 3D island growth mode (*4*). By controlling the growth process, we were able to form an atomically flat, epitaxial Ag film on GaAs(110) (*7*). The kinetic process for this epitaxy differs fundamentally from traditional epitaxial methods such as molecular beam epitaxy, where surface diffusion and surface site incorporation play central roles. In our method, the epitaxial growth requires deposition of a minimum initial thickness of Ag at a low temperature, leading to the formation of a nanocluster film. Upon subsequent annealing to room temperature, a flat epitaxial film is formed through an atomic redistribution process in which atoms in all layers participate. The basic structure of this Ag film is close-packed (111); however, it is modulated by a long-range quasi-periodic arrangement along the substrate [001] direction. The observed quasi periodicity is characterized by the "silver mean" irrationality, which has been studied extensively since the discovery of quasi crystals but has not previously been realized experimentally (*8*).

Atomically flat GaAs(110) substrates were created by cleaving GaAs bars in ultrahigh vacuum (UHV). Silver was deposited by means of a bead-on-a-filament–type evaporator (deposition rate, 0.3 to 1.5 Å/min). Silver epitaxy on GaAs(110) was studied by scanning tunneling microscopy (STM) in UHV in two ways: (i) Ag was deposited on a GaAs substrate held at low temperature (135 K) but was imaged only after it was annealed to room temperature; (ii) Ag was deposited on a GaAs substrate held at low temperature, and its temperature-dependent evolution was monitored by variable-temperature STM (*9*) while warming to room temperature.

For a nominal deposition of 15 Å of Ag at room temperature, we observed the characteristic 3D island growth morphology previously reported (*4*). The oblong-shaped clusters (Fig. 1A) are typically several hundred angstroms in length and 20 to 30 Å in height. For a similar thickness (15 Å) of Ag deposited at 135 K, the as-deposited film is composed of Ag nanoclusters that have a fairly narrow size distribution (diameter, ~2 to 3 nm) and completely cover the substrate (Fig. 1B). The formation of the nanocluster film is a direct consequence of the reduced diffusion coefficient of Ag atoms at low temperature. Upon subsequent annealing to room temperature, a perfectly flat, epitaxial, single-crystal film with a uniform thickness was formed (Fig. 1C). The film also contained small pits extending down to the GaAs substrate. From their depth, the thickness of the film was measured to be ~15 Å. Inside these pits (Fig. 1D), atomic rows with spacings exactly matching the lattice constant of GaAs (5.65 Å) were observed. Additionally, there were a few Ag clusters scattered inside the pit. Outside the pit, on the surface of the Ag film, were stripes with two characteristic spacings of ~13 and ~17 Å, forming a silver mean quasi-periodic superstructure (*8*). This feature will be discussed later.

The as-deposited Ag nanocluster film varies in thickness because of the statistical nature of the deposition process, yet the final film after annealing is atomically flat over thousands of angstroms. Apparently, all atoms must have participated in the formation of this very flat film of a particular thickness, which is termed the critical thickness (*10*). This specific thickness is so highly preferred that any deficiency results in completely empty pits. The formation of the pits also allows the determination of this critical thickness, 15 Å.

To further demonstrate the preference of the film to reach this critical thickness,

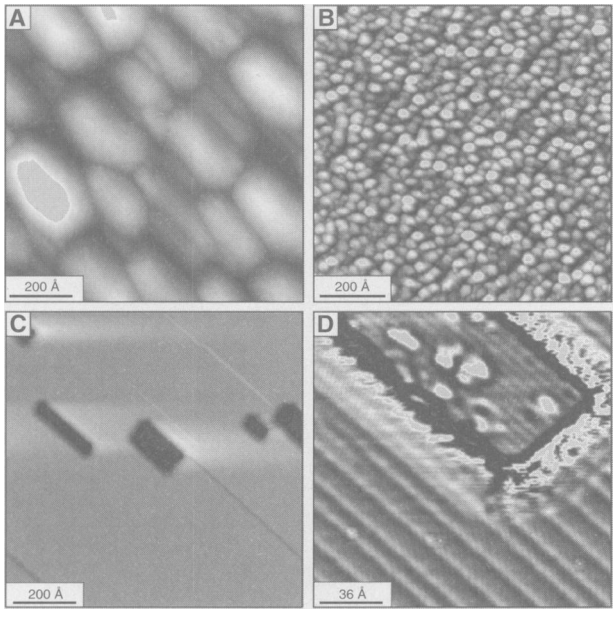

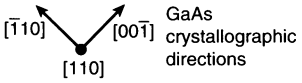

Fig. 1. (**A**) Silver 3D islands created by depositing 15 Å of Ag at room temperature (RT) on a clean GaAs(110) surface. (**B**) Low-temperature (LT) STM image (145 K) showing the nanocluster morphology. (**C**) Silver 2D film created by depositing 15 Å of Ag on a clean GaAs(110) surface at LT (135 K) and annealing the film to RT. (**D**) Curvature image of one of the pits in the film. GaAs atomic rows are seen at the bottom of the pit; the quasi-periodic superstructure is revealed at the top.

Department of Physics, University of Texas at Austin, Austin, TX 78712, USA.

*To whom correspondence should be addressed.

we performed coverage-dependent studies. When only 7.5 Å of Ag was deposited at low temperature and then annealed to room temperature, it did not form a uniform and flat film with a thickness of 7.5 Å. Instead, the film was broken into interconnected pieces (Fig. 2A) that were flattened on top and had characteristic heights of 11 to 15 Å; between these interconnected pieces were bare GaAs regions. This result further supports the idea that Ag atoms arrange themselves to form a film approaching a critical thickness; as a result of the much lower initial coverage, the connectivity of the film is reduced such that a uniform film of a single height cannot be obtained. When the initial deposition exceeded the critical thickness, the surface was completely covered by the Ag film, and the excess Ag formed 2D islands that were distributed across the surface (Fig. 2B). The coverage-dependent studies clearly establish that a flat 15 Å layer is a low–free-energy configuration.

Low-energy electron diffraction (LEED) analysis of the sample covered with flat Ag film suggested a (111)-oriented surface, and the lattice spacing of this sample was determined from the primary diffraction spots to agree closely with the value for bulk Ag(111) (*11*). In addition to the main hexagonal diffraction spots, the LEED pattern contains many fractional spots between the main spots along the k direction, in parallel to the GaAs [001] direction (Fig. 3), consistent with the superstructure modulation described in Fig. 1D. These fractional spots are not regularly spaced, and their positions between [0,0] and [1,0] do not agree with those between $[\bar{1},0]$ and $[\bar{2},0]$, which indicates that the real-space modulation is not periodic. However, the positions of these fractional spots show a well-defined hierarchy that can be expanded as linear combinations of two basic units, a and b, with integer coefficients m and n, where $a \approx 0.42$ and $b \approx 0.58$ (Fig. 3). This well-defined hierarchy of the diffraction spots signifies that there exists a well-defined real-space sequence of the quasi-periodic superstructure.

The two numbers that form the basis of the hierarchy are close (to within 1%) to the irrational numbers $1/(\sqrt{2}+1) = 0.414\ldots$ and $\sqrt{2}/(\sqrt{2}+1) = 0.585\ldots$. The denominator of these fractions can be written as a continued-fraction expansion, $2 + \frac{1}{2} + \frac{1}{2} + \frac{1}{2} + \frac{1}{2} \ldots$, which is known as the silver mean, in analogy to the well-known golden mean $(\sqrt{5}+1)/2$, which has a continued-fraction expansion of 1's. The Fibonacci sequence, the fivefold symmetric Penrose tiling, and icosahedral quasi crystals are all associated with the golden mean. The golden mean sequence, ABAAB-ABAABAAB . . . , can be formed by the iteration of $S_{n+1} = \{S_n, S_{n-1}\}$ from the seeds $S_1 = A$ and $S_2 = \{A,B\}$. The silver mean sequence can be formed by the iteration of $S_{n+1} = \{S_n, S_n, S_{n-1}\}$ from the same seeds, with the result ABABAABABAAB-ABABAABABAABABABA . . . (*10*). The real-space arrangement shows approximate agreement with such a sequence, as discussed below.

The underlying hexagonal lattice is evident from the atomic row directions (Fig. 4A). The atomic rows appear to group together, forming a chainlike structure that runs in parallel to the $[\bar{1}10]$ direction of the GaAs substrate. The apparent heights of these atomic chains are modulated by a superstructure

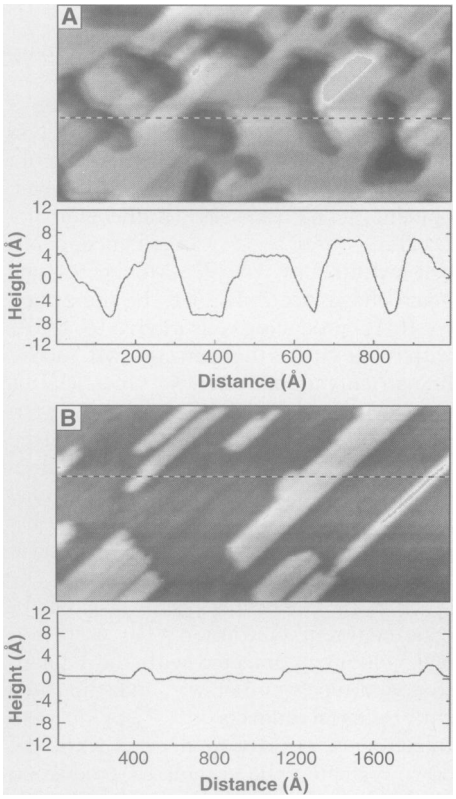

Fig. 2. (**A**) Morphology of film created by depositing 7.5 Å of Ag at LT and annealing to RT. Two characteristic mesa heights are shown in the line profile, which was taken at the dotted line in the STM image. (**B**) Flat Ag film created by depositing 22.5 Å of Ag at LT and annealing to RT. As shown in the line profile, 2D islands with single-monolayer height are scattered about the surface.

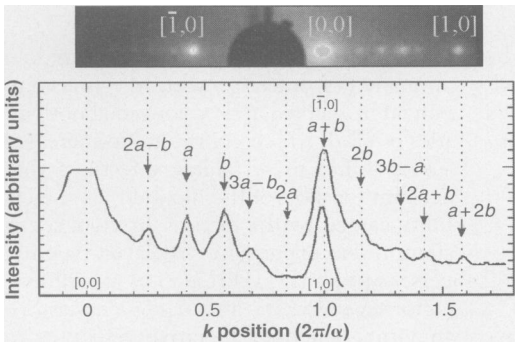

Fig. 3. LEED spots and the corresponding intensity profile along the direction of uniaxial modulation, which is parallel to the substrate GaAs [001] direction. The spots between $[\bar{1},0]$ and $[\bar{2},0]$ are folded to be between [1,0] and [2,0]. The k position is expressed in units of $2\pi/\alpha$, where α is the spacing between Ag atomic rows. All major peaks associated with the primary combination of $ma + nb$ ($a \approx 0.42$ and $b \approx 0.58$) are also marked with vertical dashed lines.

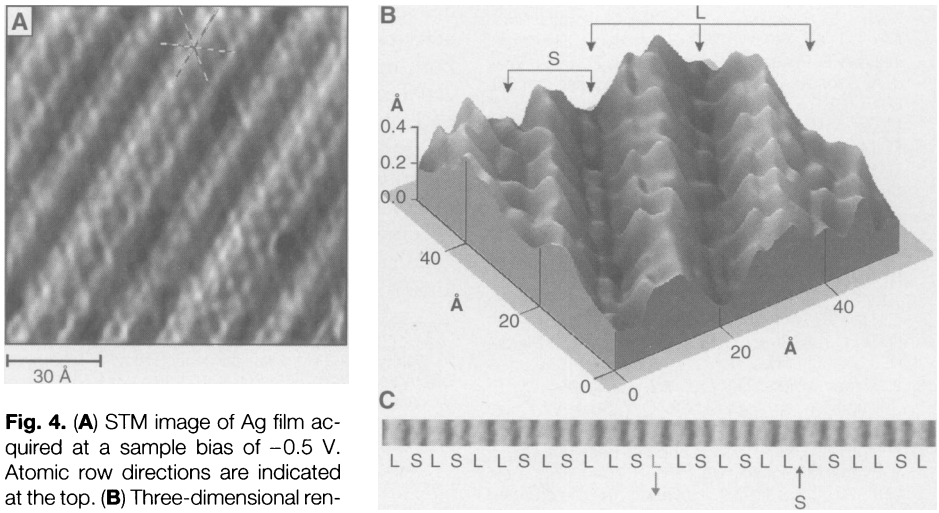

Fig. 4. (**A**) STM image of Ag film acquired at a sample bias of −0.5 V. Atomic row directions are indicated at the top. (**B**) Three-dimensional rendering of a smaller STM image; the L segment contains a double-ridge structure whereas the S segment contains a single ridge. (**C**) STM image strip (length, 390 Å) in the direction transverse to the atomic chains. This sequence exactly follows that of the silver mean except at the two defect sites, one of which is marked as an extra L segment and the other as a missing S segment.

with two characteristic spacings, one ~13 Å and the other ~17 Å, corresponding to five and seven atomic row spacings in ideal bulk Ag crystals. Using the valley of the supermodulation as the boundary, we labeled the two characteristic spacings as S (short segment) and L (long segment) (Fig. 4B). The peak of the L segment contains a double-ridge structure, whereas the peak of the S segment contains a single ridge.

Analysis of a strip of the STM image in the direction transverse to the atomic chains (Fig. 4C) shows that this sequence follows exactly that of the silver mean, except at two locations, one of which is construed as an extra L segment and the other as a missing S segment. These two locations can be considered as the positions where the silver mean sequence is broken. The average coherent length of the silver mean quasi periodicity, defined as the mean distance between the missing or extra segments, is ~100 Å.

The requirement of a sharply defined critical thickness for the formation of atomically flat metallic films and the preference for a silver mean over other types of quasi-periodic modulation remain unexplained. It is also unknown whether there is a causal relation between the existence of the critical thickness and the formation of the silver mean quasi-periodic structure. Further studies will be needed to resolve the many remaining questions surrounding this phenomenon.

REFERENCES AND NOTES

1. M. G. Lagally, *Phys. Today* **46** (no. 11), 24 (1993) and references therein; E. D. Williams and N. C. Bartelt, *Science* **251**, 393 (1991).
2. R. J. Hamers, U. K. Kohler, J. E. Demuth, *J. Vac. Sci. Technol.* **A8**, 195 (1990); Y.-W. Mo, R. Kariotis, D. E. Savage, M. G. Lagally, *Surf. Sci.* **219**, L551 (1989); R. Kunkel, B. Poelsema, L. K. Verheij, G. Comsa, *Phys. Rev. Lett.* **65**, 733 (1990); G. Rosenfeld, R. Servaty, C. Teichert, B. Poelsema, G. Comsa, *ibid.* **71**, 895 (1993); J. A. Stroscio, D. T. Pierce, R. A. Dragoset, *ibid.* **70**, 3615 (1993); J. Vrijmoeth, H. A. van der Vegt, J. A. Meyer, E. Vlieg, R. J. Behm, *ibid.* **72**, 3843 (1994).
3. R. M. Feenstra, *Phys. Rev. Lett.* **63**, 1412 (1989); C.-K. Shih, R. M. Feenstra, P. Martensson, *J. Vac. Sci. Technol.* **A8**, 3379 (1990).
4. B. M. Trafas, Y.-N. Yang, R. L. Siefert, J. H. Weaver, *Phys. Rev. B* **43**, 14107 (1991).
5. G. A. Prinz and J. J. Krebs, *Appl. Phys. Lett.* **39**, (1981); B. J. Jonker, G. A. Prinz, Y. U. Idzerda, *J. Vac. Sci. Technol.* **B9**, 2437 (1991); J. R. Waldrop and R. W. Grant, *Appl. Phys. Lett.* **34**, 630 (1979); P. N. First, J. A. Stroscio, R. A. Dragoset, D. T. Pierce, R. J. Celotta, *Phys. Rev. Lett.* **63**, 1416 (1989).
6. J. Tersoff, *Phys. Rev. Lett.* **52**, 465 (1984); W. E. Spicer, I. Lindau, P. R. Skeath, C. Y. Su, P. W. Chye, *ibid.* **44**, 420 (1980).
7. The growth process described has been used by D. A. Evans, M. Alonso, R. Cimino, K. Horn, *Phys. Rev. Lett.* **70**, 3483 (1993). However, they interpreted such a process to result in a uniform size of Ag islands (that is, quantum dots), which leads to quantum size effects in photoemission.
8. G. Gumbs and M. K. Ali, *Phys. Rev. Lett.* **60**, 1081 (1988); M. Holzer, *Phys. Rev. B* **38**, 1709 (1988).
9. A. R. Smith and C.-K. Shih, *Rev. Sci. Instrum.* **66**, 2499 (1995).
10. As used here, critical thickness has an opposite meaning to the same term in the context of pseudomorphic growth, where the epitaxial layer can only be grown up to a certain maximum critical thickness before strain relaxation occurs. For example, see J. J. Fritz, P. L. Gourley, L. R. Dawson, *Appl. Phys. Lett.* **51**, 1004 (1987).
11. Although our analysis shows close agreement, we found that there was a small shift in the position of the [0,0] beam of the Ag overlayer with respect to the [0,0] beam of the GaAs substrate. The offset angle is ~2°.

12. We thank Z. Zhang and K. Horn for useful discussions. Supported by NSF grant DMR-9402938, NSF Science and Technology Center grant CHE-8920120, and the Welch Foundation.

8 March 1996; accepted 7 May 1996

Mechanism of Suppression of Cell-Mediated Immunity by Measles Virus

Christopher L. Karp,* Maria Wysocka, Larry M. Wahl, Joseph M. Ahearn, Peter J. Cuomo, Barbara Sherry, Giorgio Trinchieri, Diane E. Griffin

The mechanisms underlying the profound suppression of cell-mediated immunity (CMI) accompanying measles are unclear. Interleukin-12 (IL-12), derived principally from monocytes and macrophages, is critical for the generation of CMI. Measles virus (MV) infection of primary human monocytes specifically down-regulated IL-12 production. Cross-linking of CD46, a complement regulatory protein that is the cellular receptor for MV, with antibody or with the complement activation product C3b similarly inhibited monocyte IL-12 production, providing a plausible mechanism for MV-induced immunosuppression. CD46 provides a regulatory link between the complement system and cellular immune responses.

Measles virus kills 1 to 2 million children annually (*1*). Infection with MV is accompanied by marked and prolonged abnormalities of CMI, which contribute to increased susceptibility to secondary infections that account for most of the morbidity and mortality caused by the disease. In vivo, sensitization and expression of delayed-type hypersensitivity (DTH) responses are inhibited for several weeks after acute measles (*2*). In vitro, lymphoproliferative responses to MV antigen, recall antigen, and mitogen are suppressed, and natural killer (NK) cell activity is markedly decreased (*3*). There is both in vivo and in vitro evidence of a type 2 polarization in cytokine responses during and after measles: Production of IL-4 is increased and production of IL-2 and gamma interferon (IFN-γ) is decreased (*4*). Immunization with live-attenuated measles vaccine produces similar abnormalities in cellular immune responses (*5*). The mechanisms responsible for the marked suppression of CMI associated with measles have remained obscure.

IL-12 is critical to the development of CMI, being (i) a potent inducer of IFN-γ from T and NK cells, (ii) co-mitogenic for T and NK cells, (iii) required for the development of Th1 responses, (iv) necessary for DTH responses, and (v) an enhancer of NK cell cytotoxicity (*6*, *7*). Monocytes and macrophages are thought to be the principal IL-12–producing cells in vivo (*6*, *8*). As with other viruses that perturb CMI, such as human immunodeficiency virus (HIV), monocytes and macrophages are prime targets of MV in natural infection (*9*). Given the close match between the abnormalities of cellular immune function seen in measles and the known functions of IL-12, we hypothesized that MV infection might down-regulate the production of IL-12.

Human monocytes were isolated by countercurrent elutriation (*10*) from normal volunteers, infected with the Edmonston wild-type strain of MV, and stimulated with bacterial inducers of IL-12 production. Infection of primary monocytes with MV down-regulated the stimulated production of IL-12, both at the level of the highly regulated p40 subunit and at the level of the functional p70 heterodimer (Fig. 1) (*11*, *12*). The suppression of IL-12 was stimulus-independent, occurring whether lipopolysaccharide (LPS) or *Staphylococcus aureus* Cowan strain 1 (SAC) was used alone (Fig. 1A) or after preincubation with IFN-γ (Fig.

C. L. Karp, J. M. Ahearn, P. J. Cuomo, Department of Medicine, Johns Hopkins University School of Medicine, Baltimore, MD 21287, USA.
M. Wysocka and G. Trinchieri, Wistar Institute of Anatomy and Biology, Philadelphia, PA 19104, USA.
L. M. Wahl, Laboratory of Immunology, National Institute of Dental Research, National Institutes of Health, Bethesda, MD 20892, USA.
B. Sherry, Picower Institute for Medical Research, Manhasset, NY 11030, USA.
D. E. Griffin, Department of Molecular Microbiology and Immunology, Johns Hopkins University School of Hygiene and Public Health, Baltimore, MD 21205, USA.
*To whom correspondence should be addressed.